NUMERICAL INVESTIGATION OF THE INFLUENCE OF WELDING PARAMETERS ON THE WELD POOL DYNAMICS AND THE DISTRIBUTION OF SECOND PHASE PARTICLES

R. KABOLI*, M. MASSOUDI FARID**, R. KRAMER*, G. ERTUGRUL* and P. MAYR*

*Chemnitz University of Technology, Germany
**Freiberg University of Technology, Germany

DOI 10.3217/978-3-85125-615-4-03

ABSTRACT

Plasma transferred arc welding (PTA) is widely used to deposit metallic materials on substrates in order to improve for example wear resistance, chemical resistance or thermal shock resistance. In terms of wear resistance, a homogeneous distribution of hard second phase particles in the deposited weld metal is favorable to achieve uniform properties. Therefore, it is important to know how the distribution of particles is affected by the welding parameters and the welding procedure in general. While experimental methods have only limited ability to provide a comprehensive insight into the weld pool dynamics, the numerical simulation of the PTA process does but is at the same time also a challenging task.
Within this work, the influence of PTA welding parameters on weld pool dynamics and distribution of second phase particles in the solidified weld metal is investigated applying thermodynamic and numerical simulation. As matrix material, a CoCr alloy (Stellite 6) is used and tungsten carbide particles are included as hard second phase. The finite volume simulation using the software package ANSYS Fluent considers several physical phenomena such as solidification/melting, magnetohydrodynamics (MHD), magnetic fields, etc. The solidification behaviour is studied using the thermodynamic software package ThermoCalc. The established numerical models solve the equations of the conservation of mass, momentum and energy by means of the Euler–Euler and Euler–Lagrange method.
Within this work, it was shown that thermodynamic and numerical simulations are valuable tools to describe weld pool dynamics as a function of different welding parameters for the PTA process. The distribution of second phase particles in a solidified metallic matrix was directly linked to the weld pool movement and can therefore be optimized. Simulation was verified by welding trials and subsequent metallographic characterisation.

Keywords: Plasma transferred arc welding, ANSYS Fluent, multiphase flow, Euler–Euler method, Euler–Lagrange method

INTRODUCTION

Plasma transferred arc welding (PTA) is one of the most useful surface modification processes. A high power plasma column is used to melt feeding material and a thin layer of substrate to form a coating layer. The coating layer is characterized by low viscosity, which is perfectly bonded to the substrate. The power density of the PTA welding (50-100 kW/cm2) takes an intermediate position between arc welding (<15 kW/cm2) and laser/electron beam welding (>100 kW/cm2) [1]. The particular characteristics of PTA welding enables it to modify the surface, which lead to achieve excellent wear and corrosion resistance whereas the toughness of the bulk material is maintained. Therefore, PTA welding provides an excellent technology to optimize the properties of materials and to improve the functionality of them. The characterization, modeling, metallurgical and microstructure analyses have been the main research interests in PTA welding. Drastic progress has been made during the past years and has been reported [2,3].

A series of Co based alloys has been developed as surface modifying materials for steel components. Stellite 6 (Co-Cr) is widely used for surface modification due to its excellent properties. The strengthening mechanisms are solid solution and precipitation hardening [4]. The properties of the surface layer can be further improved by means of the additional embedded hard particles such as tungsten carbides (WC, W2C). The strength and wear resistance can be significantly improved by adding a small amount of hard materials to the surface layer. In this research, a combination of Stellite 6 (which will act as matrix) and tungsten carbide (WC) powder were used in this experiment. A schematic of the PTA process is shown in Fig. 1. Powders are supplied by a carrier gas to form a deposit layer on the base metal. A non-transferred plasma arc (pilot arc) is initially ignited between anode and cathode in the plasma torch to achieve ionisation of the gas. Then the transferred plasma arc (main arc) is started between the base metal and the tungsten electrode and it supplies the molten powders to the base metal. Thereby, a thin and dense coating layer with low dilution is generated on the base metal.

Because of the importance of film formation, several researchers have developed various models to predict film formation and relevant quantities [6,7]. Most of these models are valid for thin films. None of these models can be applied for the thick film modelling where 3D flow inside the film needs to be captured. A pure VOF approach can be used for modelling 3D flow inside the film. However, modelling these tiny droplets using pure VOF approach would need a very large number of mesh elements and is thus beyond the scope of practical computation limits. In this work, a lagrangian particle is tracked by a Discrete Phase Model. As this particle reaches the melting temperature, it is converted to an eulerian droplet using a User Defined Function (UDFs) in ANSYS Fluent. This droplet is further tracked in an Eulerian frame-work using a Euler-Euler model. This hybrid DPM-to-Euler-Euler approach enables taking the advantages of both the basic lagrangian and eulerian models into account. The DPM model, which is computationally less intensive, takes care of the particle movement in the bulk of the domain and the more accurate model Euler-Euler models takes care of the resulting droplet.

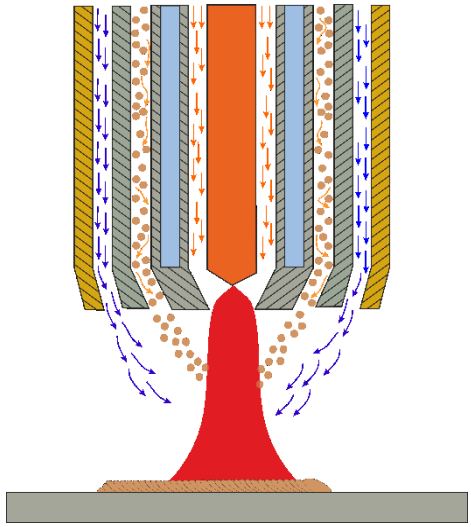

Fig. 1 The schematic of the PTA process.

NUMERICAL MODEL

The goal of this research project is the investigation of the physical phenomena such as heat and mass transfer, electromagnetic and hydrodynamic processes in PTA welding with multi-metal powders and the estimation of their influence on the weld bead formation by methods of numerical simulation. The number of different physics involved in PTA makes its simulation challenging especially when all four states of matter namely solid, liquid, gas and plasma must be considered and numerous physical phenomena interact together.

To solve such a complex model, the problem is divided into two sub-models. The first model covers the formation of plasma. The second model was developed to investigate the injection and the tracking of particles, melting and solidification as well as the formation of the weld bead (see Table 1).

Table 1 sub-models and the modules

Plasma model	**Particle trace and melt model**
Electric currents	Particle injection
Magnetic field	Particle tracing
Joule heating	Particle melting
Laminar flow	Laminar flow
Heat transfer	Heat transfer
Magnetohydrodynamic (MHD)	Melting and solidification

PLASMA MODEL

The Plasma model was developed in the simulation software COMSOL. The computation domain is shown in Fig. 1. The welding arc is formed between the tungsten electrode and the steel workpiece. The Direct Current Electrode Negative (DCEN) polarity is used, therefore the tungsten electrode is the cathode and the steel workpiece is the anode. The computation domain and the boundary conditions are shown schematically in Fig. 2.

The plasma model is based on the following assumptions:

- The computation domain is axially-symmetric
- The problem is solved in steady state since the arc enters into steady state just after arc formation
- The arc is stationary and under atmospheric pressure
- Gas flow is laminar and incompressible
- The arc plasma is in Local Thermodynamic Equilibrium (LTE)
- Metal vapors are not taken into account
- Gas properties change only with the temperature
- Debye sheath are not considered

GOVERNING EQUATIONS

In the steady state and under axial-symmetric conditions, the governing equations, which describe arc plasma motion, are as follows:

Mass conservation:

$$\frac{\partial}{\partial z}(\rho.u_z)+\frac{1}{r}\frac{\partial}{\partial r}(\rho.r.u_r)=0 \tag{1}$$

Radial momentum conservation:

$$\frac{1}{r}\frac{\partial}{\partial r}(\rho.r.u_r^2)+\frac{\partial}{\partial z}(\rho.u_r.z)\ = \\ -\frac{\partial P}{\partial r}+\frac{1}{r}\frac{\partial}{\partial r}\left(2r\mu\frac{\partial u_r}{\partial r}\right)+\frac{\partial}{\partial z}\left(\mu(\frac{\partial u_z}{\partial z}+\frac{\partial u_r}{\partial r}\right)-2\mu\frac{u_r}{r^2}-j_zB_\theta \tag{2}$$

Axial momentum conservation:

$$\frac{1}{r}\frac{\partial}{\partial r}(\rho.u_r.u_z)+\frac{\partial}{\partial z}(\rho.u_z^2)\ = \\ -\frac{\partial P}{\partial z}+\frac{\partial}{\partial z}\left(2\mu\frac{\partial u_z}{\partial z}\right)+\frac{1}{r}\frac{\partial}{\partial r}\left(r\mu(\frac{\partial u_z}{\partial r}+\frac{\partial u_r}{\partial z}\right)-j_iB_\theta \tag{3}$$

Energy conservation equations:

$$\frac{1}{r}\frac{\partial}{\partial r}(r.\rho.C_P.u_r.T)+\frac{\partial}{\partial z}(\rho.C_P.u_z.T)= \\ \frac{1}{r}\frac{\partial}{\partial r}\left(rk\frac{\partial T}{\partial r}\right)+\frac{\partial}{\partial z}\left(k\frac{\partial T}{\partial z}\right)+\frac{J_z^2+J_r^2}{\sigma}+\frac{5k_B}{2e}\left(J_r\frac{\partial T}{\partial r}+J_z\frac{\partial T}{\partial z}\right)-U \tag{4}$$

Where subscripts r and z denote radial and axial directions, respectively. The terms in the planes are special momentum and energy source terms concerning with plasma. In equations 1-4, the basic variables defined are temperature T, pressure P, radial velocity u_r and axial velocity u_z. The plasma property functions are densityρ, viscosityμ, specific heat C_P, thermal conductivity k and electrical conductivity σ [5]. The current density components and the magnetic inductive intensity required in Eq. 2, 3. and 4 are obtained by Maxwell's equations described in the magnetic vector potential format:

$$E = -\nabla\varphi - \frac{\partial A}{\partial t} \tag{5}$$

$$B = \nabla \times A \tag{6}$$

Where E, φ, B, A are electrical field vector, electrical potential, magnetic inductive intensity vector, and magnetic vector potential. Under the steady state and axially symmetric conditions, the governing equations can be derived as:

Current continuity equations:

$$\frac{1}{r}\frac{\partial}{\partial r}\left(r.\sigma.\frac{\partial\varphi}{\partial r}\right) + \frac{\partial}{\partial z}\left(\sigma.\frac{\partial\varphi}{\partial z}\right) = 0 \tag{7}$$

Ampere's law ($\mu_0 = 4\pi \times 10^{-7}$)

$$\frac{1}{r}\frac{\partial}{\partial r}\left(r\frac{\partial A_z}{\partial r}\right) + \frac{\partial}{\partial z}\left(\frac{\partial A_z}{\partial z}\right) = \mu_0.j_z \tag{8}$$

$$\frac{1}{r}\frac{\partial}{\partial r}\left(r\frac{\partial A_r}{\partial r}\right) + \frac{\partial}{\partial z}\left(\frac{\partial A_r}{\partial z}\right) = \mu_0.j_r \tag{9}$$

$$j_z = -\sigma\frac{\partial\varphi}{\partial z} \tag{10}$$

$$j_r = -\sigma\frac{\partial\varphi}{\partial r} \tag{11}$$

For converting A to B necessary in Eq. 5 and 6, a component of Eq. 6 is written as:

$$B_0 = \frac{\partial A_r}{\partial z} - \frac{\partial A_z}{\partial r} \tag{12}$$

Thermodynamic properties and the transport coefficients of argon are taken from the COMSOL database. After it, the modules, which are mentioned in table 1, were coupled to solve the problem.

This numerical model is based on the Bauchire et al.'s model [5]. As mentioned in their work, the equations are highly non-linear. Attention must be paid for initiating and reaching convergence. An initial temperature of 10,000 K or greater must be set to ensure that the gases are fully ionized to reach convergence in the numerical solution. After solving the

plasma model, the calculated temperature and velocity fields were imported as input for the second model.

PARTICLE TRACE AND MELT MODEL

The discrete phase model (DPM) with a lagrangian approach coupled with a Volume of Fraction (VOF) approach was applied to trace particles and melt in ANSYS Fluent. Particles were tracked in lagrangian frame as point sources. Two-way coupling was used to simulate the energy and momentum exchange with eulerian gas phase (Fig. 3). The DPM model is ideally suited for situations where particles enter and leave the computational domain. The discrete parcels of particles were uniformly distributed and injected through the powder inlet at each time step. Each parcel was tracked separately. The DPM model is suitable for dilute particulate flow when the particle mass fraction is lower than 10%.

After the injection of particles in the domain, some of the particles were heated up to melting temperature and were molten and some of them which have not reached the melting temperature were still considered as lagrangian particle. The molten particles were deleted from the Euler-Lagrange frame and imported to the Euler-Euler frame via a user defined function (UDF) in ANSYS Fluent. In order to simulate phase interfaces of particles, the Euler-Euler method was used.

As mentioned earlier, Euler-Euler method has been used in this work, which is the most complex of the multiphase models in ANSYS Fluent. It solves a set of n momentum and continuity equations for each phase. Coupling is achieved through the pressure and interphase change coefficients. The melting temperature, melting enthalpy and heat capacity of Stellite and tungsten carbide have been calculated via the thermodynamic software ThermoCalc and imported in ANSYS Fluent as input.

EXPERIMENTAL SETUP

A welding robot equipped with a plasma torch was used to carry out experimental investigations. In order to validate the simulation results, thermocouples were welded on top of the metal sheet to capture the temperature during the welding process (Fig. 2).

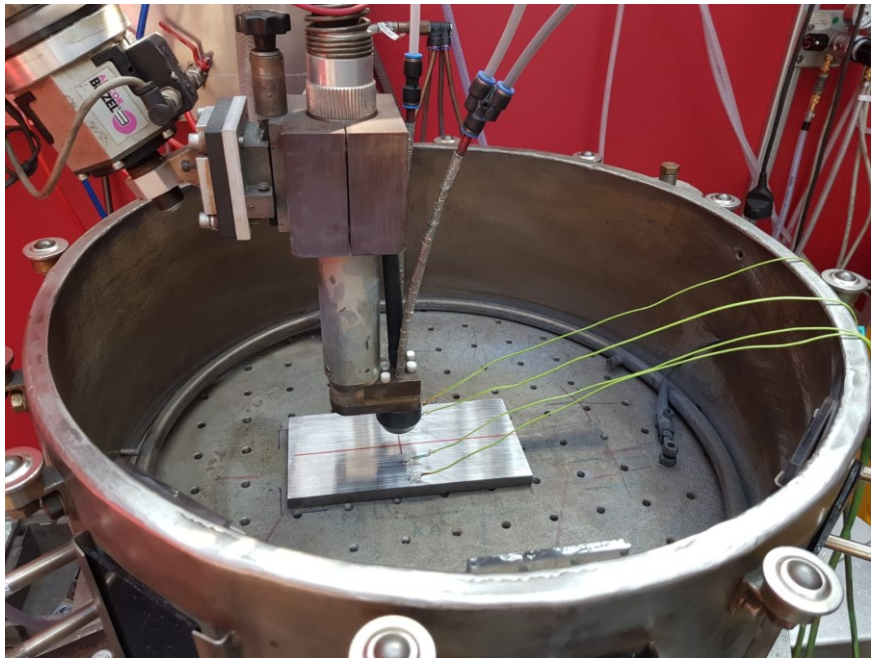

Fig. 2 The experimental setup.

RESULTS AND DISCUSSION

In order to have a better understanding of the PTA process and to explain the experimental results, a CFD-Model was developed using the commercial software COMSOL and ANSYS Fluent.

The following welding conditions were assumed in the model: a current density of 1e8 [A/m^2], a minimum value sigma min of 1 [s/m] in the argon region and the plasma gas and shielding gas flow rate is fixed to 2 L/min and 8 L/min, respectively.

Figures 3 and 4 show the temperature and velocity fields under steady state conditions inside the arc plasma and the simulation domain. The maximum temperature of 12000 K and the maximum velocity of 7 m/s were observed.

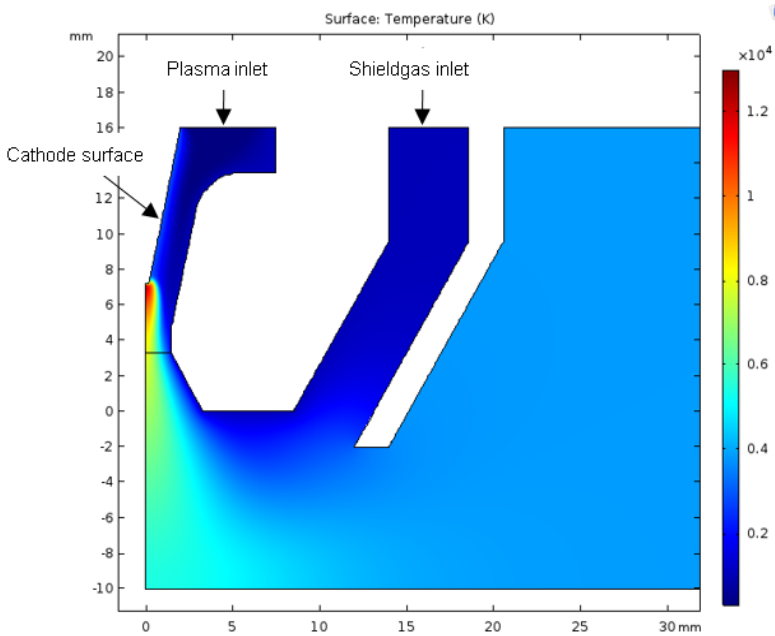

Fig. 3 Calculated temperature fields in COMSOL.

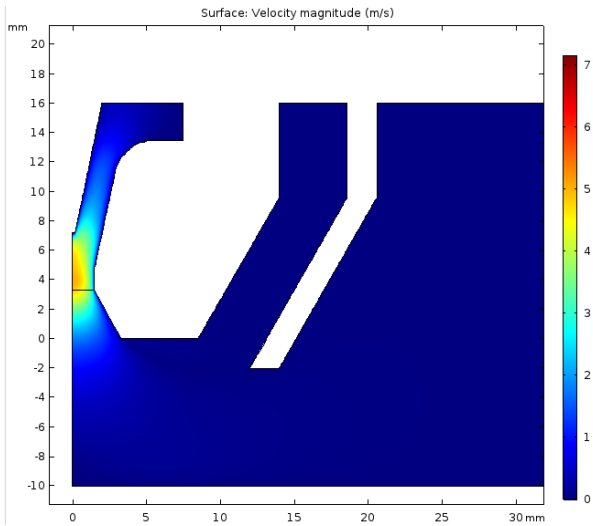

Fig. 4 Contours of velocity magnitude fields in COMSOL.

These results were imported to ANSYS Fluent to simulate particle tracking and melting. A wide range of material/physical properties affected the particle melting. Among material properties and process conditions, melting rate of the particle, wetting angle, surface tension at the interface and viscosity were the main affecting parameters. Unfortunately, most of these parameters were unknown for Stellite 6 and WC. Therefore, some estimated values were used in the model. The particle temperature is shown in figures 5a and 5b at various times. It shows that the particles which reached the melting temperature were dissolved

from the Euler-Lagrange domain and added to the Euler-Euler domain. It also shows that some particles, which did not reach the melting temperature, left the domain which was observed by experimental investigations (Fig 6).

The weld bead after solidification and phase fraction of Stellite and tungsten carbide are shown in Figure 7. They are in agreement with numerical results (Fig 8).

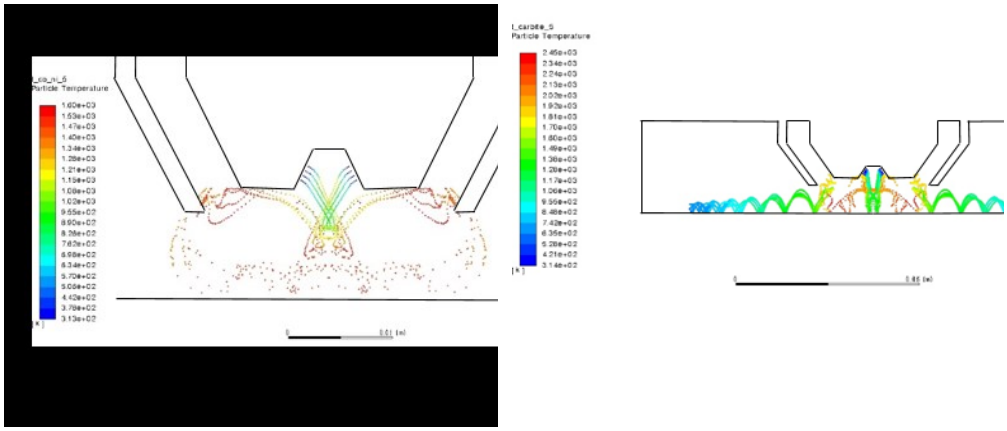

Fig. 5a and 5b particle temperature of Stellite (left) and WC (right).

Fig. 6 unmolten particles on the surface of the test plate.

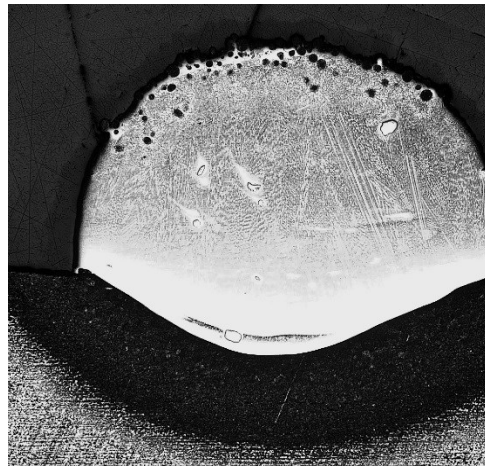

Fig. 7 weld bed after 10 seconds.

It was observed that the value of the surface tension between phases and wetting angle between phases and the bottom edge of domain had a very big influence on the shape of the welding bead. The values of these parameters need to be studied via experimental investigations.

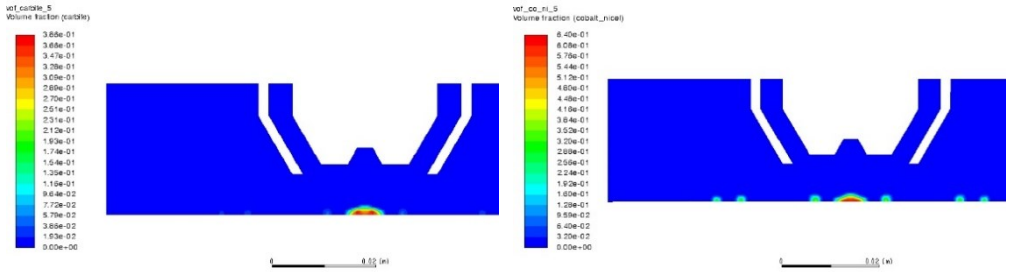

Fig. 8 phase fraction of WC (left) and Stellite 6 (right).

Figure 9 shows the velocity and temperature fields of argon. The velocity field under the plasma column is affected by the molten particles as expected. The model predicts the effect of melting enthalpy of the temperature fields correctly.

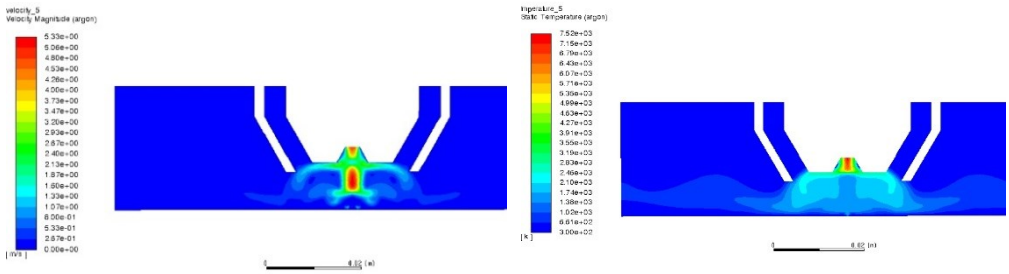

Fig. 9 velocity (left) and temperature fields (right) after 10 seconds.

CONCLUSIONS

In this paper, a heat transfer and fluid flow model for PTA welding is presented. This model can explain the phenomena particle melting and weld pool shape formation. Gravity, electromagnetic forces, arc pressure and Marangoni effect were taken into account.

The DC plasma torch was modeled by developing a 2D axisymmetric model of laminar flow and heat transfer, coupled with the electromagnetic field. Lorentz force and joule heating effects were modeled, coupled with the physical model of the plasma torch. In order to ensure that the electric flow was ensured, an artificial minimum value of 8000 S/m for the electrical conductivity of argon was used. The numerical results of the gas temperature and axial velocity results were quite satisfactory, although more complete reproductions of the thermal and fluid phenomena might be obtained with three-dimensional modelling. In that case, computational requirements and computing times should be also taken into account.

A multi-phase flow model was established, and ANSYS Fluent was applied to simulate the multi-phase flow for gaining significant insight into understanding of particle melting and phase distribution bead formation mechanism. Melting rate of the particle, wetting angle, surface tension at the interface and viscosity were the main affecting parameters and must be set carefully. The calculation results were reasonable and reliable. It can be

concluded that the presented CFD method is a powerful approach to investigate mechanisms of the PTA process

ACKNOWLEDGEMENTS

The authors gratefully acknowledge the funding by the German Research Foundation (Deutsche Forschungsgemeinschaft, DFG) within the project MA 5861/6-1 “Process-oriented modeling and simulation of unsteady modulated gas flows in plasma powder cladding to influence layer properties”.

REFERENCES

[1] S.H. KANG, T. SHINODA, Y. KATO and H.S. JEONG: ‘Thermal Fatigue Characteristics of PTA Hardfaced Steels’, Surface Engineering, Vol. 17, No. 6, pp. 498-504, 2001.

[2] P.F. MENDEZ, N. BARNES, K. BELL, S.D. BORLE, S.S. GAJAPATHI, S.D. GUEST, H. IZADI, A.K. GOL, and G. WOOD: ‘Welding processes for wear resistant overlays’, Journal of Manufacturing Processes, Vol. 16, pp. 4-25, 2014.

[3] S.H. NIKAM, N.K. JAIN, and S. JHAVAR, and G. WOOD: ‘Thermal modeling of geometry of single-track deposition in micro-plasma transferred arc deposition process, Journal of Materials Processing Technology, Vol. 230, pp. 121-130, 2016.

[4] J.L. ACEVEDO-DÁVILA A, R. MUÑOZ-ARROYO A, H.M. HDZ-GARCÍA A, A.I. MARTINEZ-ENRIQUEZ B, M. ALVAREZ-VERA A and F.A. HERNÁNDEZ-GARCÍA: ‘Cobalt-based PTA coatings, effects of addition of TiC nanoparticles’, Vacuum, Vol. 143, pp. 14-22, 2017.

[5] J. BAUCHIRE, J. M. GONZALEZ and A. GLEIZES: ‘Modeling of a DC Plasma Torch in Laminar and Turbulent Flow’, Plasma Chemistry and Plasma Processing, Vol. 17, No. 4, pp. 409-432, 1997.

[6] J. SENDA and H. Fujimoto: ‘Multidimensional modelling of impinging sprays on the wall in diesel, ASME, 2009.

[7] R. SCHMEHL, R. ROSSKAMP, and S. WITTING: ‘CFD analysisof spray propagation and evaporation including wall film formation and spray/film interactions’, Internation journal of heat and fluid flow, Vol. 20, No. 5, pp. 520-529, 1999.